MASS TRANSFER AT A MOVING PARTICLE IN A FLUIDIZED BED OF COARSE MATERIAL

G. I. Pal'chenok and A. I. Tamarin

UDC 66.096.5

An experimental study has been made of mass transfer to a moving particle in the fluidized bed of coarse inert material. The experimental results are presented in terms of dimensionless relationships.

Low-temperature combustion in a fluidized bed (FB) involves the use of crushed solid fuel in a layer of large ($d_i \geq$ 1-2 mm) inert particles. The process is operated in the transitional range [1], where the burning rate is determined to a considerable extent by the rate of oxidant supply to the particles.

The literature carries extensive information on the mass transfer between particles and gas in FB, but the data were obtained under conditions where all the particles in the bed participate [2-5]. On the other hand, the fuel concentration is only 1-3% on combustion in an FB. Measurements have been made [6, 7] on the mass transfer for naphthalene particles in an FB composed of inert polymer material having the same density and grain size. As the fuel particles may differ considerably in size and density from the incombustible ones, the result is not of general significance. In [8], measurements were made on the mass transfer for a single coke particle burning in an FB. The value of the results obtained for the range $Ar \leq 6 \cdot 10^4$ was reduced somewhat by the fact that the experiments were performed with a small column (diameter 40 mm).

Here we have examined the mass transfer to a moving particle in an FB composed of coarse inert material, in which we varied the sizes and densities of the active and inert particles over wide ranges and examined the effects from the hydrodynamic and scale factors.

The experiments were performed in a lucite column of diameter 0.15 m. The initial height of the bed was also 0.15 m, the bed consisting of the materials whose characteristics are given in Table 1. The bed was fluidized with air, the flow rate being measured from the pressure difference across a standard diaphragm. The bed temperature was maintained at 50°C by heating the air in an electric system.

The probe mobile particle was injected into the bed at the same temperature. This particle was a sphere bearing a layer of naphthalene and was suspended on a thin filament, which allowed it to move freely throughout the volume of the bed. The probe diameter varied from 3.5 to 30 mm, and the effective density varied from 400 to 2500 kg/m^3. The probe was weighed on an analytical balance before and after the experiment. From the loss of naphthalene in the FB, we determined the mean-mass transfer coefficient. The run time (5 min) was close to the actual burning times for real fuel particles in FB and was much greater than the circulation period in the bed (~1-10 sec). This enables one to consider the process as quasistationary and to calculate the mass-transfer coefficient from

$$\frac{\beta}{RT_w}(P_w - P_f) = \frac{\Delta m}{\tau F}. \quad (1)$$

The naphthalene vapor content in the incident air was $P_f = 0$, and therefore the driving force for the transfer is $(P_w - P_f) = P_w$. The partial pressure of the naphthalene vapor (P_w) is a single-valued function of surface temperature. The surface acquired the bed temperature almost instantaneously because of the preheating and the high rate of heat exchange, and that temperature was used in calculating P_w from the formula of [9]. The error in determining β from (1) was not more than 6%.

Lykov Institute of Heat and Mass Transfer, Academy of Sciences of the Belorussian SSR, Minsk. Translated from Inzhenerno-Fizicheskii Zhurnal, Vol. 47, No. 2, pp. 235-242, August, 1984. Original article submitted April 19, 1983.

 0022-0841/84/4702-0916$08.50

TABLE 1. Characteristics of Dispersed Materials

№	Material	d_i, mm	ρ_i, kg/m³	φ
1	Glass spheres	1,3	2500	1,0
2	Grains of millet	2,0	1200	0,96
3	Worn crushed firebrick	2,0	2350	0,8
4	Peas	6,2	1340	1,0

There may be a certain contribution to the loss of naphthalene from abrasion and adsorption by the bed particles. Special measurements [10, 11] have shown that the abrasion of naphthalene specimens in FB is negligible at 40-60°C by comparison with the convective mass transfer, and the same applies to the adsorption of naphthalene by the particles. In our measurements, the probe moved along with the bed material, and therefore the relative velocity and hence the abrasion should not be greater than that with the specimen fixed, as in the experiments described above. As according to [12] the contribution from abrasion to the mass loss is about 3%, the values of β calculated from (1) were reduced by 5% with a certain safety margin.

Figure 1 shows typical relationships between the mass-transfer coefficient and the gas infiltration rate. The performance in mass transfer increased with the mean bed particle diameter (curves 1 and 4 in Fig. 1a and c) and also with the density of those particles (curves 1 in Fig. 1b and c). An increase in probe diameter (curves 1 and 2 in Fig. 1a and curves 1 and 2 in Fig. 1d) or a reduction in density (curves 2 and 3 of Fig. 1c) reduced β. The mass-transfer coefficient was also almost independent of the infiltration rate. Only near the start of fluoridization was β somewhat reduced for large heavy probes (curve 3 of Fig. 1a), while for large light probes it increased with the gas speed (curve 3 of Fig. 1b). In both cases with $u \geq 1.3u_0$ the mass-transfer coefficient stabilized. The form of the $\beta = f(u)$ curves is related to the motion of the probe, which may be judged from observations on the upper boundary and the region near the wall, as well as from characteristic collisions of the probe on the grating. The observations showed that relatively small probes ($D_p/d_i \leq 7$) participated in the circulation, periodically rising to the surface and descending again. Here the less dense probes spent much of the time in the upper part of the bed, as was evident from their more frequent appearance on the surface. Relatively large and heavy probes ($8 < D_p/d_i$; $\rho_p/\rho_i = 0.5$-2.0) rested on the grating at speeds close to u_0. For $u \geq 1.3u_0$, large probes close in density to the bed material ($\rho_p/\rho_i = 0.5$-1.2) begin to be lifted up by rising bubbles, to judge from the frequency of collisions with the grid, which causes β to fall and stabilize (curve 3 of Fig. 1a). Heavier probes ($\rho_p/\rho_i = 1.7$-2.0) remained on the grid even at high gas speeds, merely rolling about or lifting slightly. Large but light probes ($8 < D_p/d_i$; $\rho_p/\rho_i = 0.2$-0.35) floated at the surface of the bed at speeds close to u_0. As the speed increased ($u \geq 1.3u_0$), they were entrained in the circulation, which increased and stabilized the mass-transfer coefficient (curve 3 of Fig. 1b).

The mass-transfer coefficient for mobile active particles is thus independent of the infiltration rate (for large probes with $\rho_p/\rho_i \leq 1.2$ at $u > 1.3u_0$), which indicates that they spend most of their time in the emulsified phase of the bed, where the two-phase theory [2, 4] indicates that the gas speed and porosity on average correspond to the conditions for the start of fluidization. Therefore, the mass transfer for an active particle should be determined by u_0. The relative size and density of the particle affect the motion, so the experimental data were plotted in accordance with the function

$$\frac{\mathrm{Sh}}{\mathrm{Sc}^{1/3}} = f\left(\mathrm{Re}_0, \frac{D_p}{d_i}, \frac{\rho_p}{\rho_i}, \varphi\right). \quad (2)$$

The numbers Sh and Re_0 are based on the natural internal linear scale of the FB: the bed particle size d_i.

As the inert particles were both spherical and irregular, (2) includes the form factor φ, which is equal to the ratio of the surface of a sphere of the same volume to the surface of the particle. The experimental data (over 450 points) were processed by computer using multiparameter regression analysis [13] on the basis of a power law. Here we neglected the data corresponding to large heavy probes lying on the grid and also large light ones floating at the surface. This gave the following correlation:

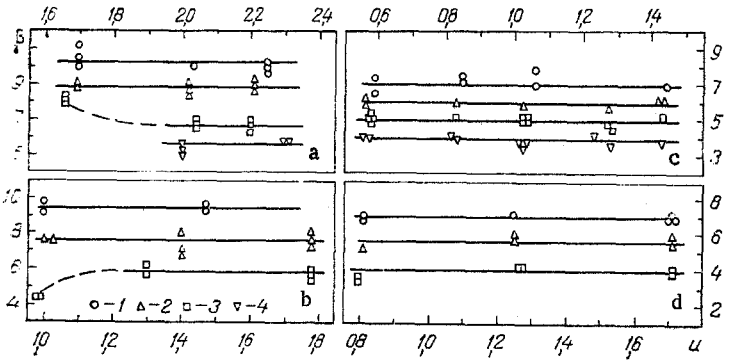

Fig. 1. Experimental $\beta = f(u)$ curves: a) FB of peas (1-4 correspondingly D_p/ρ_p = 4.5/2000, 7.2/2000, 26.5/1150, 28.1/350 mm/kg/m^3); b) firebrick FB (1, 2, 3 — D_p/ρ_p = 4.2/2000, 7.5/1300, 17.1/800 mm/kg/m^3); c) millet grain FB (1, 2, 3, 4 — D_p/ρ_p = 4.2/2000, 16.3/1400, 17/700, 29/350 mm/kg/m^3); d) glass sphere FB (1, 2, 3 — D_p/ρ_p = 6.4/2100, 14.3/2100, 30/450 mm/kg/m^3); β and u in m/sec.

$$\frac{\mathrm{Sh}}{\mathrm{Sc}^{1/3}} = 0{,}925\mathrm{Re}_0^{0.65}\left(\frac{d_i}{D_p}\right)^{0.13}\left(\frac{\rho_i}{\rho_p}\right)^{-0.15}. \qquad (3)$$

Figure 2 compares calculations from (3) with experiment. The mean relative error in the correlation is 8%, which is close to the accuracy in measuring the mass-transfer coefficient. Table 2 gives the ranges for the variables appearing in (3) and the standard errors of the corresponding powers (regression coefficients). It is evident from (3) that the form of the inert particles did not affect the mass-transfer rate within the range examined. (The exponent φ does not differ reliably from zero.)

In [6, 7], the concentration profile of the naphthalene vapor was measured over the height of the bed to examine the mass transfer from naphthalene particles in an inert FB for the particular case $D_p = d_i$, $\rho_p = \rho_i$, which gave

$$\frac{\mathrm{Sh}}{\mathrm{Sc}^{1/3}} = 0{,}04\mathrm{Re}_0 + 2{,}12\mathrm{Re}_0^{0.41} + 0{.}62\mathrm{Re}_0^{-0.51}. \qquad (4)$$

According to (4), the mass transfer is also determined only by the speed at which fluidization starts. Figure 3 compares the correlation of (3) for $D_p = d_i$, $\rho_p = \rho_i$ with (4), which indicates that in our range $45 \leqslant \mathrm{Re}_0 \leqslant 600$ the two are virtually the same (the maximum discrepancy is 10%, which corresponds to the accuracy of each of the correlations). The similarity between the data obtained by different methods indicates that the relationship of (3) is reliable. The diameters of these systems in [6, 7] were 47, 66, and 94 mm, while in our case the diameter was 150 mm, which indicates that the mass-transfer coefficient is independent of the scale.

Also, there was no effect on the mass transfer from varying the concentration of active particles in the FB from 1.5 to 10% [6, 7]. The data obtained under these conditions were virtually the same as those for single particles, which shows that our local simulation method is sound and also indicates that adjacent active particles do not influence one another at low concentrations.

In [3] we find an observed relationship for the mass exchange between phases in a stationary bed of spheres at $\mathrm{Re}_e > 30$, which was also obtained by local simulation:

$$\mathrm{Sh}_e = 0{,}395\mathrm{Re}_e^{0.64}\mathrm{Sc}^{1/3}. \qquad (5)$$

The Sh_e and Re_e of (5) are based on the equivalent diameter d_e of a channel between grains and the mean gas speed u/ε in it. On transforming to Sh and Re and taking porosity $\varepsilon_0 \approx 0.4$ as characteristic of the emulsified phase, we get from (5) that

$$\mathrm{Sh} = 0{,}95\mathrm{Re}^{0.64}\mathrm{Sc}^{1/3}. \qquad (5a)$$

Equations (5a) and (3) are virtually the same for $D_p = d_i$, $\rho_p = \rho_i$, which indicates that the laws of mass transfer are common to stationary and fluidized beds of large particles. The emulsified phase in an FB, where active particles predominate, may be considered as a

TABLE 2. Ranges in the Variables Appearing in (3) and Standard Errors of the Corresponding Exponents (regression coefficients)

Variable	Range	Standard error
Re_0	45—600	±0,007
Ar	$1,5 \cdot 10^5$—$8,6 \cdot 10^6$	±0,004
D_p/d_i	0,59—23,0	±0,01
ρ_p/ρ_i	0,14—2,1	±0,01

stationary bed with mean values for the porosity and infiltration rate that determine the mass transfer close to ε_0 and u_0.

The exponent to Re_0 in (3) is higher than that for pure laminar flow, evidently because of the mode of flow around the particles in the transitional range in Re_0 that was used, namely the production of vortices in the root zone [3, 14], which is responsible for additional circulation transport at the active particles.

Convective mass (heat) transfer is closely related to the hydrodynamic resistance in laminar flow [14] and in turbulent flow [15]. The relationship in its simplest form (for Sc = 1) is expressed by the Reynolds analogy, which for flow in a channel takes the form

$$St = Sh/ReSc = \zeta/8. \quad (6)$$

It is suggested [15] that the factor $Sc^{-2/3}$ should be introduced on the right in (6) for $Sc \neq 1$. In that form, the analogy is obeyed closely for Sc of 0.6-3000. In [16], the hydrodynamic analogy was extended to detached flow.

If we consider the emulsified phase in an FB as a stationary bed with mean porosity and infiltration rate ε_0 and u_0 we have that the resistance to the rising gas flow in the FB is equal to the weight of the particles when allowance is made for the Archimedean force [2-4] and is independent of the infiltration speed. From the viewpoint of an interior problem on gas flow in a bed, one has flow through a channel of equivalent diameter d_e and mean length H_0T, and we can put [3]

$$\Delta P = \zeta \frac{H_0 T}{d_e} \frac{\rho}{2} \left(\frac{u_0 T}{\varepsilon_0} \right)^2 = (1 - \varepsilon_0)(\rho_i - \rho) H_0 g. \quad (7)$$

We expand the expression for d_e by substituting $u_0 = Re_0 \nu/d_i$ in (7) and using the fact that T = 1.5 as indicated by experiment, while $\varepsilon_0 = 0.4$ characteristically for FB [3], which gives

$$\zeta = 2.53 \cdot 10^{-2} \frac{Ar}{Re_0^2}. \quad (8)$$

We use Todes's interpolation formula relating Re_0 and Ar [3], which agrees well with experiment, and then (8) enables one to calculate the dependence of the resistance coefficient ζ on Re_0. Curve 1 of Fig. 4 shows the results, together with the experimental curves $\zeta = f(Re)$ of [3] for a disordered stationary layer of spheres with $\varepsilon = 0.3019$ and 0.476, which have been redrawn in the new coordinates. In the range used in Re_0, the calculated $\zeta = f(Re_0)$ relationship for an FB is approximated by the following power law with maximum deviations of ±10%:

$$\zeta = 7.0\, Re_0^{-0,35}. \quad (9)$$

The $\zeta = f(Re)$ curves for stationary beds are approximated with about the same accuracy by functions that differ from (9) only in numerical factors.

We substitute (9) into (6) to get for $Sc \neq 1$

$$Sh = 0.875\, Re_0^{0,65}\, Sc^{1/3}. \quad (10)$$

Relationship (10), which is derived from the hydrodynamic theory of heat and mass transfer, essentially coincides with (3) for $D_p/d_i = \rho_p/\rho_i = 1$; if the mobile particle differs in size and density from the bed particles, an additional cofactor appears in (3) to correct for

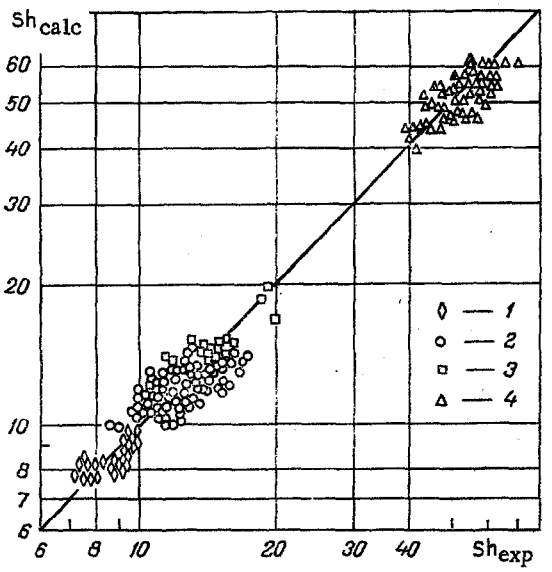

Fig. 2. Comparison of calculations from (3) with experiment: 1-4) correspondingly for the data on layers 1-4 in Table 1.

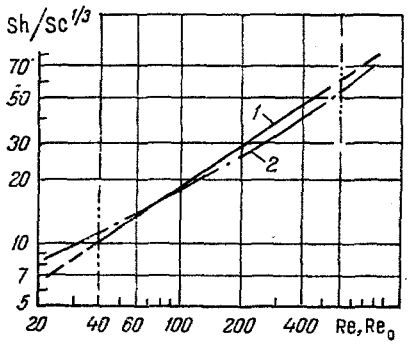

Fig. 3

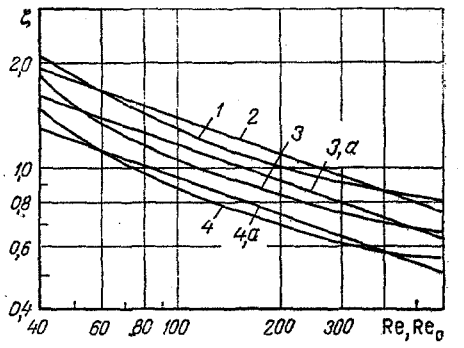

Fig. 4

Fig. 3. Calculated dependence of $Sh/Sc^{1/3}$ on Re_0 ($d_i = D_p$, $\rho_i = \rho_p$): 1 and 2) correspondingly from (3) and (4).

Fig. 4. Dependence of the resistance coefficient $\zeta = \Delta P\,(d_e/l)(2\varepsilon^2/\rho u^2)$ on a Reynolds number: 1, 2) by calculation from (8) and (9) for FB; 3, 4) experimental relationships for a stationary layer for $\varepsilon = 0.3019$ and 0.476 (Fig. 2.32 of [3]); 3a, 4a) power-law approximations correspondingly for (3) and (4) of the form $\zeta \sim Re^{-0.35}$.

the effects of the individual parameters of the mobile particle. The form of the dependence of Sh on Re_0 is not altered, which means that the mass transfer is still determined by the flow around the inert particles and the formation of the related gas flow pattern at the exchange surface. However, the local structural characteristics near that surface such as the porosity may differ from those averaged over the emulsified phase.

As Re_0 is a function of Ar [3], it is more convenient to use the latter in practical calculations, as it is calculated directly from the properties of the bed and gas. Then the experimental data on mass transfer for a mobile particle in an FB were fitted by regression analysis to Sh = f(Ar):

$$\frac{Sh}{Sc^{1/3}} = 0.117\,Ar^{0.39}\left(\frac{d_i}{D_p}\right)^{0.13}\left(\frac{\rho_i}{\rho_p}\right)^{-0.15}. \qquad (3a)$$

The mean relative error in the correlation of (3a) is 7.8%. We see from (3) and (3a) that on transferring from Re_0 to Ar, the correction for the individual properties of the mobile particle is unaltered.

We note that the mass-transfer coefficients for immobile heavy large probes (ones lying on the grating), which were not incorporated in the treatment, were on average 30% higher than those calculated from (3) and (3a), while those for particles floating at the surface were lower by 10-15%. This enables one to estimate the mass transfer under such conditions. In the first case, there is obviously an effect from the hydrodynamic circumstances near the grid, while in the second there is a reduction in the effective flow speed for the probe emerging on the surface.

This study of mass transfer for a mobile particle in an FB has been used with published experimental relationships to relate the mass transport to the type of gas motion in the emulsion phase. It is found that the mass-transfer rate is determined by the speed for the onset of fluidization and is independent of the gas infiltration speed and apparatus scale. The correlations (3) and (3a) incorporates the effects of the sizes and densities of the active and inert particles, and also those of the gas properties, and they can be used to calculate buring rates for solid fuel in fluidized-bed ovens.

NOTATION

D, diffusion coefficient for naphthalene vapor in air: D_p, experimental mean diameter of active particle (probe); d_i, mean particle diameter; d_e, equivalent diameter of channels; F, probe surface; g, acceleration due to gravity; H, bed height; l, channel length; P_f, P_w, partial pressures of naphthalene vapor in the incoming air flow and at the probe surface; R, gas constant of naphthalene vapor; T, channel tortuosity coefficient; T_w, absolute temperature of the probe surface; u, gas infiltration velocity (referred to the cross section of the empty apparatus); β, mass-transfer coefficient; Δm, decrease in mass; ΔP, pressure drop in the bed; ε, bed porosity; ζ, resistance coefficient; ρ, ρ_i, ρ_p, density of gas, bed material, and effective density of the probe; ν, kinematic viscosity; τ, residence time; φ, shape factor for bed particles; Ar, Archimedes number; Re_e, Reynolds number; Sh, Sherwood number; Sc, Schmidt number; St, Stanton number. Subscripts: 0, minimum fluidization; calc, predicted; exp, experimental.

LITERATURE CITED

1. P. Basu, "Burning rate of carbon in fluidized beds," Fuel, 56, No. 4, 390-391 (1977).
2. S. S. Zubrodskii, Hydrodynamics and Heat Transfer in a Fluidized Bed [in Russian], Gosénergoizdat, Moscow (1963).
3. M. E. Aerov and O. M. Todes, The Hydraulic and Thermal Principles of Equipment with Stationary and Fluidized Granular Beds [in Russian], Khimiya, Leningrad (1968).
4. J. F. Davidson and D. Harrison (eds), Fluidization, Academic Press (1971).
5. N. I. Syromyatnikov, L. K. Vasanova, and Yu. N. Shimanskii, Heat and Mass Transfer in a Fluidized Bed [in Russian], Khimiya, Moscow (1967).
6. T. H. Hsiung and G. Thodos, "Mass transfer in gas-fluidized beds: measurement of actual driving forces," Chem. Eng. Sci., 32, No. 6, 581-592 (1977).
7. T. H. Hsiung and G. Thodos, "Transitional mass-transfer behavior from packed-bed conditions to onset of fluidization," Int. J. Heat Mass Transfer, 22, No. 7, 1003-1008 (1979).
8. A. I. Tamarin et al., "A study of convective transfer between a burning particle and a fluidized bed," in: Heat and Mass Transfer VI [in Russian], Vol. VI, Part 1, ITMO im. A. V. Lykova Akad. Nauk BSSR, Minsk (1980), pp. 44-49.
9. I. A. Gil'denblat, A. S. Furmanov, and N. M. Zhavoronkov, "The vapor pressure over crystalline naphthalene," Zh. Prikl. Khim., 33, No. 1, 246-248 (1960).
10. A. P. Baskakov and V. M. Suprun, "Determination of the convective component in the heat-transfer coefficient for a gas in a fluidized bed," Khim. Neft. Mash., No. 3, 20-21 (1971).
11. M. N. Markova, "Mass transfer by evaporation from the surface of a body immersed in a fluidized bed of fine-grain material," Doctoral Dissertation, Moscow (1972).
12. E. N. Ziegler and I. T. Holmes, "Mass transfer from fixed surfaces to gas fluidized beds," Chem. Eng. Sci., Vol. 21, No. 2 (1966), pp. 117-122.
13. Collection of FORTRAN Scientific Programs: Programmer's Handbook [in Russian], Issue 1, Statistika, Moscow (1974).
14. H. Schlichting, Boundary Layer Theory, McGraw-Hill (1968).

15. T. K. Sherwood et al., Mass Transfer, McGraw-Hill (1975).
16. L. I. Kudryashov, "Extension of the hydrodynamic theory of heat transfer to the case of flow around bodies with detachment," Izv. Akad. Nauk SSSR, Otd. Tekh. Nauk, No. 9, 1309-1316 (1953).

RELATIVE CORRESPONDENCE METHOD AND ITS APPLICATION IN MEASUREMENT PRACTICE

V. I. Gudkov and V. P. Motulevich

UDC 536.2:536.5

The fundamental possibilities of applying an approximate method of calculating physical processes — the relative correspondence method — to the indirect measurement of quantities are analyzed. Practical examples are given.

The fundamental propositions of the relative correspondence method were formulated in [1, 2]. The effectiveness of its application for approximate calculations of physical processes was illustrated on the solution of a number of practical problems [1-3]. Further analysis of the method showed, however, that the feasibility of its use is not confined to the circle of theoretical–calculation problems but also extends to the region of measurement practice [4].

Quantities are measured indirectly in the majority of cases in engineering and scientific research. The unknown physical quantity y, dependent on several quantities, is defined by the general equation

$$y = i(x_1, x_2, \ldots, x_p) + \beta I(x_1, x_2, \ldots, x_l), \tag{1}$$

where $i(x_1, x_2, \ldots, x_p)$ and $I(x_1, x_2, \ldots, x\zeta)$ are the measured quantities or functions of these quantities. The expression (1) is written so as to isolate a certain parameter or complex

$$\beta = f(x_1, x_2, \ldots, x_j, \ldots, x_k), \tag{2}$$

the determination of which is difficult under the measurement conditions. The latter may be a consequence of the fact that it is impossible to measure the quantity β directly, while for its calculation or extrapolation there is either an approximate or an exact but very complicated relation. In a number of cases such difficulties prove to be surmountable using the relative correspondence method.

The essence of this method consists in the following: In the determination of relative quantities with a given degree of confidence it is possible to use a less precise model of the process than in the determination of absolute quantities.

Let us initially consider β as a function of one argument x_j,

$$\beta = f = f(x_j). \tag{3}$$

We assume that a simplified model relation

$$\beta \approx \varphi = \varphi(x_j) \tag{4}$$

exists for β and that the initial quantity

$$f_0 = f(x_{j0}) \tag{5}$$

is known sufficiently exactly for the initial value (favorable for the calculated or experimental determination of β) of the argument x_{j0}. Then the approximate value φ* of the parameter (complex) β is determined by the calculating formula

$$f \approx \varphi^* = f_0 \frac{\varphi}{\varphi_0}, \tag{6}$$

G. M. Krzhizhanovskii State Scientific-Research Power Institute, Moscow. Moscow Power Institute. Translated from Inzhenerno-Fizicheskii Zhurnal, Vol. 47, No. 2, pp. 242-250, August, 1984. Original article submitted September 20, 1982.

 0022-0841/84/4702-0922$08.50